

**Research article**

## **Characteristics of soil erosion in different land-use patterns under natural rainfall**

**Lei Wang<sup>1,2,†</sup>, Huan Du<sup>3,†</sup>, Jiajun Wu<sup>2</sup>, Wei Gao<sup>2</sup>, Linna Suo<sup>1</sup>, Dan Wei<sup>1</sup>, Liang Jin<sup>1</sup>, Jianli Ding<sup>1</sup>, Jianzhi Xie<sup>2,\*</sup> and Zhizhuang An<sup>1,\*</sup>**

<sup>1</sup> Institute of Plant Nutrition , Resources and Environment, Beijing Academy of Agricultural and Forestry Sciences, Beijing 100097, China

<sup>2</sup> College of Resources and Environmental Sciences, Agricultural University of Hebei, Baoding, Hebei 071000, China

<sup>3</sup> Sichuan Water Conservancy College, Chengdu, Sichuan 610000, China

**\* Correspondence:** Emails: xianzhi@126.com, anzzly@126.com.

**†** These two authors contributed equally.

**Abstract:** Land degradation due to soil erosion is a major problem in mountainous areas. It is crucially important to understand the law of soil erosion under different land-use patterns with rainfall variability. We studied Qingshuihe Watershed in the Chongli district of the Zhangjiakou area. Four runoff plots, including caragana, corn, apricot trees, and barren grassland, were designed on the typical slopes of Xigou and Donggou locations. The 270 natural rainfall events observed from 2014 to 2016 were used to form a rainfall gradient. The relationship between runoff and sediment yield was analyzed. Results showed that the monthly rainfall of the slope runoff plot in the Chongli mountain area presented the trend of concentrated rainfall in summer, mainly from June to September, accounting for 82.4% of the total rainfall in 2014–2016, which was far higher than that in other months. Starting from April to May every year, the rainfall increased with time, then from July to September, the rainfall decreased gradually, but it was still at the high level of the whole year. Among the four ecosystems, the caragana-field has the best effect on reducing the kinetic energy of rainfall and runoff, which can effectively reduce the runoff and sediment yield of the slope and reduce the intensity of soil erosion. In terms of the total amount of runoff and sediment, the runoff and sediment yield of the caragana-field reduced by 74%–87% and 64%–86% compared with that of

the grassland. Comparing different land-use types, the caragana plantation would be conducive to conserving soil and water resources.

**Keywords:** Qingshuihe watershed; natural rainfall; characteristics of soil erosion

## 1. Introduction

Soil erosion is a major problem in mountainous areas. It not only causes the deterioration of land and water resources but also constrains the agricultural production system [1]. Soil erosion is a slow process that goes unnoticed for a long time, or it can happen at an alarming rate during heavy rains by causing serious topsoil loss [2,3]. Many studies showed that nutrient loss due to rainfall was one of the major concerns involved in non-point source pollution and land degradation [4,5]. The impact of raindrops on the soil surface can disperse aggregate material and break-down soil aggregates. Raindrop splash and runoff water can easily remove lighter aggregate materials like very fine sand, silt, clay, etc, and greater raindrop energy or runoff amounts can remove heavier aggregate materials. The higher the intensity of a rainstorm, the greater the erosion potential [6,7].

An estimated 25 to 40 billion tonnes of surface soil and 10 million  $\text{hm}^2$  of agricultural land eroded due to soil erosion, resulting in an economic loss of about 80\$ billion dollars [8]. Each year, soil erosion in China causes the loss of approximately five billion tonnes of topsoil and 67 thousand  $\text{hm}^2$  of cultivated land [9,10].

The vegetation cover significantly reduces runoff and soil erosion. However, the degree of soil erosion varies in relation to topographic, edaphic, and vegetative characteristics [11]. Shi et al. Studied that the greater the rainfall energy, the higher the content of fine particles in the sediment separated from the soil, which can absorb more nutrients and pollutants [12]. Fiener et al. [13] show that land-use causes changes in erosion and sediment interception capacity by changing vegetation cover, soil properties, runoff rate, and topographic conditions, and then affects erosion and sediment yield. Driven by soil erosion, carbon, and nitrogen transformation and greenhouse gas emissions may affect global climate change, but the degree of impact varies with rainfall, terrain, vegetation, soil and human management [14,15]. She et al. [16], studied field slope land-use patterns and found that the mixed vegetative pattern was more effective in intercepting the slope runoff than the single-use plot and the annual erosion modulus of a caragana and alfalfa fields was the lowest. Through the dynamic monitoring of canopy interception of caragana and apricot tree forests, the rainfall interception law of different vegetation types and the applicability of the model simulation were verified. Increased caragana canopy and greater planting densities resulted in higher canopy interception and in lower runoff and soil loss [17]. At the same time, Wang et al. [18] reported that herbaceous vegetation coverage has a profound impact on rainfall erosion dynamics and finally has a greater impact on slope runoff. In a comparative study of different land-use patterns, Zhao et al. [19] explored that the soil and water conservation effect of farmland was poor, and the effect of forestland and grassland on soil and water conservation was significant.

In China, the research on soil and water loss of slope land is mainly focused on the Loess Plateau and the Loess Hilly areas in the south, but the information related to the northern mountain areas is still limited. Particularly, in the Zhangjiakou area, defined by mostly rough terrain, elevations increase from southeast to northwest. Topographically the area is divided into three parts, including

plateau, mountains, and basin. The area has a monsoon, continental semiarid climate, with hot, humid summers and long, cold, dry, and windy winters. The sandstorms often occurred [20]. Many afforestation ecological program, such as converting cropland to forests and Three North Shelterbelt Forest Project, has resulted in a significant change in regional land use pattern [21]. Therefore, exploring the response of hydrological processes and understanding the law of soil erosion under different land-use patterns with rainfall variability is critically important.

In this study, our objectives were to determine soil erosion through runoff under different land-use patterns with rainfall variability and determine which vegetation cover is effective in conserving soil and water resources.

## 2. Materials and methods

### 2.1. Study area

Qingshuihe watershed is located in Chongli District, Zhangjiakou area, a typical mountainous basin (Figure 1). Hydraulic erosion is the main erosion characteristic [22]. Qingshuihe river flood season has the characteristics of rapid fluctuation, large peak discharge, and short duration. The vegetation coverage in the upper reaches of Qingshuihe watershed is low, the river channel gradient is large, the current is turbulent, and the soil erosion is serious. The suspended load sediment transport accounts for 54% of the total amount of Zhangjiakou station, which is the primary source of sediment in Qingshuihe watershed. The erosion modulus of the river basin is 500–10000 t/(km<sup>2</sup>·a). Qingshuihe watershed, which involves Guanting reservoir and Beijing Zhangjiakou 2022 Winter Olympic Games bid site, is an important flood control/ecological safety barrier, water supply channel, and water source protection area in the capital. Soil erosion caused the destruction of land and water resources in the study area and severely affected agricultural production and the imbalanced ecosystem.

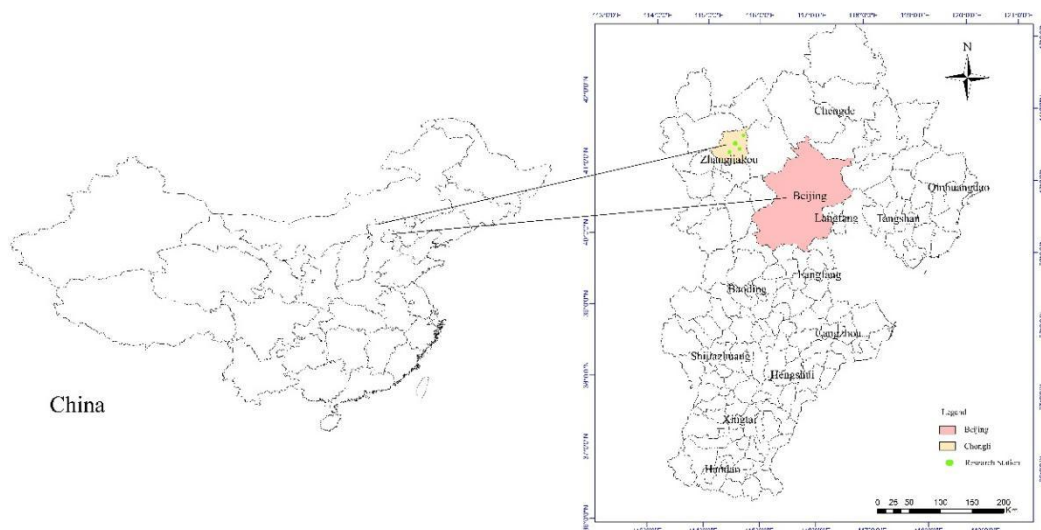




**Figure 1.** Location map of the study area and runoff plot real map.

## 2.2. Experiment design

### 2.2.1. Runoff plots

**Table 1.** Basic information of runoff plots.

Land-use	GPS		Altitude	Slope (°)	Coverage
	Longitude	Latitude			
Caragana-field	115°10'00.2"	40°58'44.6"	1250.0	20	40%
Corn-field	115°09'44.3"	40°57'20.1"	1166.2	3	45%
Apricot-field	114°57'18.6"	40°56'18.1"	932.1	20	35%
Grassland	115°10'00.4"	40°58'44.6"	922.5	20	13%

The natural rainfall experiment in this study is located in Qingshuihe watershed of Chongli District, Zhangjiakou. Based on the investigation of this area, representative land use patterns were selected, and runoff plots were designed to study the characteristics of soil erosion. The basic physical and chemical properties of soils in the four plots were basically the same. Respectively, Soil pH 7.34, organic matter 26.38 g/kg, total nitrogen 1.88 g/kg, available phosphorus 25.94 mg/kg, available potassium 219.47 mg/kg. The basic information of the runoff plot is shown in Table 1.

The caragana, corn, apricot, and grassland runoff plots were 5 m wide and 10 m long, and the

horizontal projected area was  $49 \text{ m}^2$ . In order to block the impact of the surrounding environment, it was necessary to set a 2 m wide protective belt around the runoff plot group. The dike of the runoff plot was built with cement brick; the thickness of cement brick was 0.05 m. To prevent the rainwater carried by cement brick from entering the community, the edge treatment was adopted after the completion to prevent the rainwater on the cement ridge from entering the community. The ridge was 20 cm higher than the ground, and the buried depth was 30 cm. To prevent the small area from being squeezed and collapsing, a retaining wall made of cement brick was set under the collecting trough. The retaining wall was aligned with the middle line of the plots, and the diversion pipe passed through it [23,24]. The collecting channel was constructed directly below the runoff area. The collecting channel was made of cement bricks, and the joint was filled with cement to prevent water flow or sediment from entering the gap and increasing the error. A  $1 \text{ m}^3$  impervious cement pool was constructed under the residential area as a catchment basin to receive runoff and sediment. When the rainfall was low, the collecting bucket with a scale mark was placed in the collecting basin to make the experiment more accurate. The collecting barrel was cylindrical, and the collecting basin was cubic [25,26]. The water inlet hole was set by the water pipe with a diameter of 50mm at the top of the collecting bucket and the collecting basin, and the drainage hole was set at the bottom. The PVC pipe was used for diversion between the collecting tank and the tank, and the joint was sealed with strong glue to prevent water from being soaked out. After sampling, the remaining runoff and sediment from the collecting bucket and collecting basin were discharged into the artificial pit, and the drain outlet was sealed with a plug for the next sampling record. Each collecting basin was equipped with a board to seal the collecting basin, which was covered in the collecting basin to prevent rainwater from entering into the collecting basin directly and increase the error of the next test (Figures 2a and 2b).

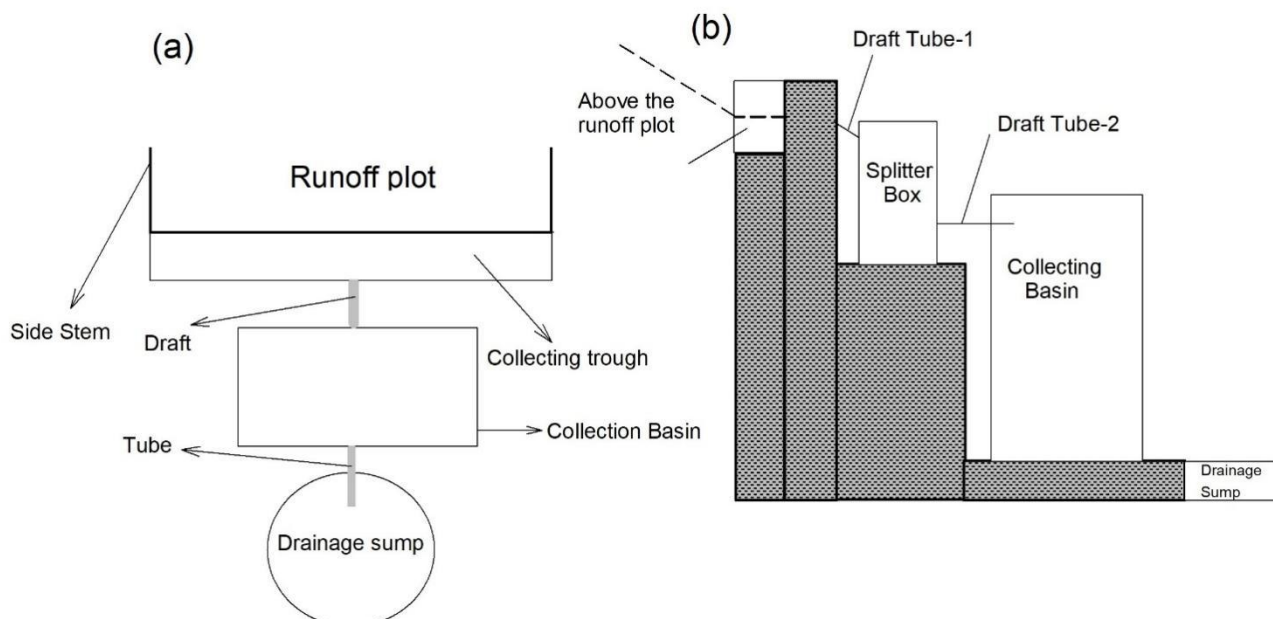


**Figure 2.** Layout of plots (a) and schematic diagram of catchment system in runoff plot (b).

### 2.2.2. Collection and treatment of water and sediment samples

The method of routine collection and measurement of runoff was adopted. After the rainfall, the inner diameter flow of the collecting bucket was recorded, the slurry in the collecting bucket was evenly mixed, and the samples were mixed at the upper, middle, and lower levels. Then, put the mixed water sample into two 500 ml sampling bottles, one for measuring runoff and the other for measuring sediment.

### 2.2.3. Determination of runoff and sediment samples

At the end of rainfall, the collected sediment samples in the bucket were sealed and kept for 24 hours to allow sediment to settle and prevent water evaporation. Then the clarified water in the collecting bucket was poured into the container, and then the volume of the water was measured and recorded. The sediment precipitated from the lower part of the collecting bucket was dug out and put into the aluminum box for weighing and recording, and then put into the oven for 105 °C drying to constant weight, and then calculated.

### 2.2.4. Dynamic observation of runoff and sediment yield

The runoff and sediment yields were relatively dense; each person was responsible for collecting a set of data, including real-time flow data recording, water, and sediment sample collection, dynamic change of slope morphology, and preparation of test tools. Since the rainfall collected does not last for a long time. Therefore, a sample is collected every 5 minutes until the runoff stops.

### 2.2.5. Vegetation coverage and slope measurement methods

The visual estimation method was used to divide the sample plots into several grids and estimate the average vegetation coverage of each grid. For slope measurements, the geological compass model was ZX/DQL-11.

## 2.3. Statistical analysis

The regression and t-tests were applied using SPSS18.0 software. Significant differences among runoff plots were determined at  $P<0.05$  through the All-pairwise comparison method. SigmaPlot 10.0 was used to visualize the data graphically.

## 3. Results

### 3.1. Characteristics of natural rainfall

#### 3.1.1. Rainfall classification

In this paper, the time interval of 1-hour was used to divide the rainfall. If the rainfall value was

not monitored for more than 1-hour, then it was regarded as two rainfall processes. The rainfall interval of less than 1-hour was considered the same rainfall. According to Table 2, all rainfall in Chongli District of Zhangjiakou area from 2014 to 2016 was classified, and its distribution characteristics are shown in Table 3. There were 80 rainfalls in 2014, 98 in 2015, and 92 in 2016. There were 270 rainfall events in three years with four variabilities: light rain, moderate rain, heavy rain, and rainstorm. Among them, 46 heavy rain and rainstorm events accounted for 17.0% of the total, while 224 events of moderate rain and light rain accounted for 83.0% of the total (Tables 2 and 3).

**Table 2.** Rainfall classification standard.

Grade	Rainfall period	
	12-hour rainfall (mm)	24-hour rainfall (mm)
Micro rainfall	<0.1	<0.1
Light rain	0.1–4.9	0.1–9.9
Moderate rain	5.0–14.9	10.0–24.9
Heavy rain	15.0–29.9	25.0–49.9
Rainstorm	30.0–69.9	50.0–99.9
Downpour	70.0–139.9	100.0–249.9
Torrential rain	≥140.0	≥250.0

**Table 3.** Rainfall grade distribution characteristics.

Year	Distribution	Rainstorm	Heavy rain	Moderate rain	Light rain	Total
2014	Rainfall frequency	7	13	12	48	80
	Total number of sessions (%)	8.8	16.2	15.0	60.0	100
2015	Rainfall frequency	2	9	18	69	98
	Total number of sessions (%)	2.0	9.2	18.4	70.4	100
2016	Rainfall frequency	4	11	20	57	92
	Total number of sessions (%)	4.3	12.0	21.7	62.0	100
Total	Rainfall frequency	13	33	50	174	270
	Total number of sessions (%)	4.8	12.2	18.5	64.5	100

### 3.1.2. Rainfall distribution characteristics

The monthly rainfall of the slope runoff plot in the Chongli mountain area presented the trend of concentrated rainfall in summer, mainly distributed in June, July, August, and September, accounting for 82.4% of the total rainfall, which was far higher than other months. From April to May every year, the rainfall increased with time, and from June to September, the rainfall gradually decreased, but it was still at the high level of the whole year (Figure 3).

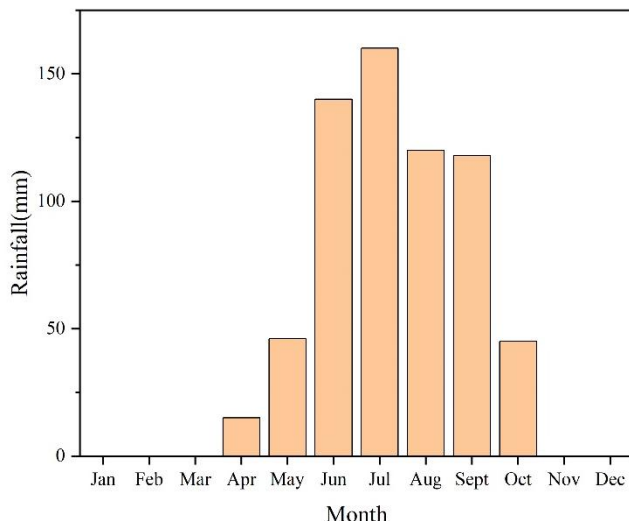


**Figure 3.** Distribution characteristics of average monthly rainfall.

### 3.2. Analysis of runoff and sediment yield process of slope surface under heavy rain

Heavy rain was recorded on 15-July 2016. The slope runoff rate of the four plots has a corresponding good relationship with the rainfall intensity in the whole rainfall process, showing an increasing and decreasing trend with the increase or decrease of rainfall intensity. The soil on the slope was relatively dry because there was no rainfall a few days before the heavy rain. When the rainfall started, the soil infiltration rate was high, and because of the influence of vegetation coverage, the runoff occurrence times of the four plots were different. The runoff of caragana-field appeared 80 minutes after the beginning of rainfall. After the rainfall intensity reached its peak, the runoff rate reached the peak at 9:10 time, which was 1.3 L/minutes. Then, the rainfall potential and its intensity changed, and the runoff rate also showed a similar trend until the end of the rainfall. Compared with the caragana-field, the runoff rate of corn plot was 25 minutes late. After the rainfall intensity peaked, the runoff rate peaked at 8:50 and 9:10, respectively, which were 2.1 L/minutes and 1.8 L/minutes, respectively.

Runoff was generated in the apricot plot about 30 minutes after the beginning of rainfall. The variation trend of rainfall intensity reached the peak at 8:05, 8:50, and 9:10, which were 46 mm/h, 55 mm/h, and 48 mm/h, respectively. Then the rainfall intensity decreased, and the change was stable until the end of the heavy rain. The runoff rate of grassland started at 8:00, compared with the rest of the runoff plots. In the whole process of rainfall, there were three peaks, which were 2.6 L/minutes at 8:25, 2.8 L/minutes at 8:35, and 4.8 L/minutes at 8:50. The grassland coverage reached 75%. After the beginning of rainfall, the runoff velocity was faster because of the larger rainfall intensity and relatively large slope, and the infiltration capacity of the soil was not reflected in time. With the continuous rainfall, the runoff began to increase, and this part of runoff belongs to infiltration. The soil basically reached the steady infiltration stage, and then with the continuous change of rainfall intensity, the runoff rate showed a corresponding change trend.

It can be seen from Figures 4a and 4b that the time of sediment yield and runoff occurrence was the same in the four plots, indicating that runoff is the carrier of sediment production. During continuous rainfall, the runoff rate and sediment yield rate also changed greatly when the rainfall intensity changed. The maximum sediment concentration occurrence time was a little later than the

wave crest in this rainfall process. On the one hand, it takes time for confluence; on the other hand, it was due to a “chain reaction” in the later period of heavy rain to produce more serious soil erosion. The gradual decrease of rainfall intensity reduced the slope sediment yield, and the sediment yield rate tends to be stable. Because of the staggered root system, the caragana-field can effectively regulate the runoff, increase the soil erosion resistance and reduce the sediment yield rate more, and the time of runoff and sediment production obviously lags behind, but after the rainfall intensity reaches a certain value, it led to the peak value of runoff and sediment yield. In the late stage of heavy rain, the rainfall intensity decreased gradually, and the runoff and sediment yield rates decreased obviously. Overall, the runoff and sediment yield of caragana-field was still lower than that of grassland in the same rainfall process. Due to the broad coverage of corn leaves, corn can effectively reduce the kinetic energy of runoff and reduce the sediment carrying capacity of runoff so that the sediment yield rate is much lower than that of grassland, and the time of runoff and sediment production was obviously lagging. However, when the rainfall intensity reached a certain value, it led to the peak value of runoff and sediment yield. While, in the same rainfall process, the total runoff and sediment yield was still lower than that of the caragana-covered plot. There were four peaks in the sand yield rate of the grassland plot, which reached the peak at 8:15, 8:35, 8:50, and 9:10, which were 1.2 g/minutes, 2.8 g/minutes, 4.8 g/minutes, and 2.7 g/minutes, respectively. At 8:00 minutes, the sediment yield did not appear at the beginning of runoff, indicating that grassland cover intercepted and filtered the sediments in the runoff during this period. After 8:10 minutes, the changing trend of sediment yield and runoff rates was similar.

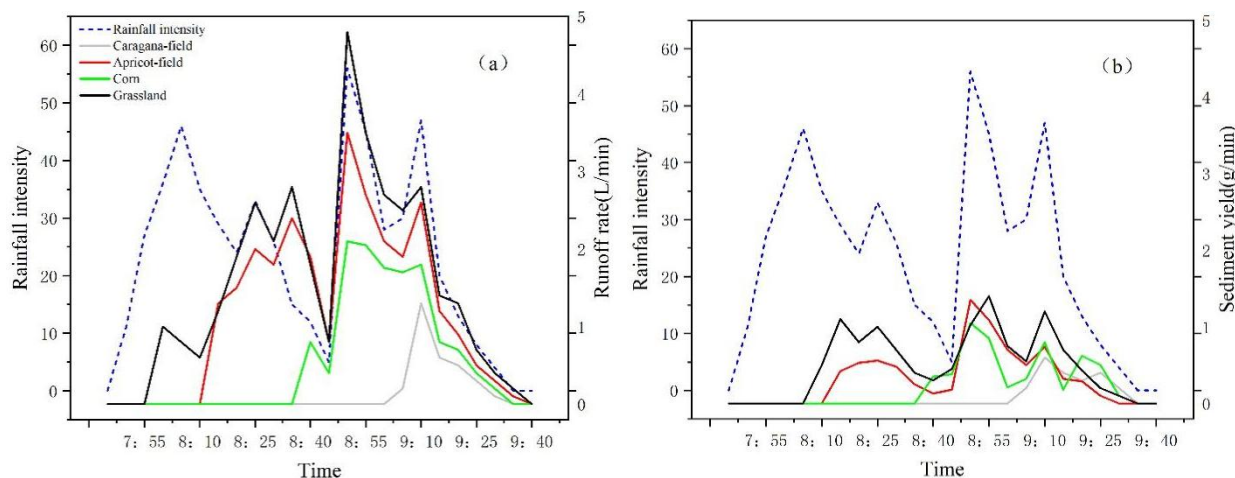


**Figure 4.** Variation characteristics of rainfall intensity and runoff rate (a) and sediment yield rate (b).

### 3.3. Analysis of runoff and sediment yield in different runoff plots

As shown in Table 4, the duration of runoff occurrence in each plot was longer than that in the sediment production calendar. The impact force of runoff became smaller at the beginning and end of runoff, and the ability to erode sediment gradually weakened. In terms of runoff and sand production time, it was the highest in the grassland. In terms of total runoff and sediment yield, the runoff rates were grassland > apricot > corn > caragana, and the sediment yields were grassland > corn > apricot > caragana. The runoff and sediment yield of grassland are 7.8 and 7.3 times that of caragana field, 3.1 and 1.9 times that of corn plot, and 2.6 and 2.2 times that of apricot field. The main reason

could be that the caragana has strong soil and water conservation capacity, which can effectively intercept the impact of rainwater on the soil. The developed root system of caragana tree can absorb maximum precipitation and reduce surface runoff. Because of its special geographical position, the corn plot is different from traditional farmland. Its cultivated area is not exposed. Rainfall mainly splashes the soil around the corn. At the same time, rainfall passes through the top of the corn to form a concentrated water flow, which strengthens the splash ability. However, the splash area is restricted. Therefore, compared with the traditional farmland, this cultivation method of corn is more conducive to reducing soil erosion and protecting soil erosion.

**Table 4.** Runoff and sediment yield characteristics of runoff plots under heavy rainfall.

Land-use	Duration of runoff generation (minutes)	Calendar time of sand production (minutes)	Production flow (L)	Sediment yield (g)
Caragana-field	30	25	22.87	9.07
Corn	50	45	57.75	35.10
Apricot-field	80	70	69.36	29.70
Grassland	100	90	179.30	66.15

### 3.4. Analysis of runoff and sediment yield process of slope surface under moderate rain conditions

Moderate rain was recorded on 20-June 2016. In moderate rain conditions, the rainfall duration was long, and the average rainfall intensity was small, so the runoff rate of the four plots was low. The caragana plot had the late runoff occurrence time, followed by the apricot ecosystem and grassland had the earliest runoff time. At the same time, the corn plot was produced 40 minutes later than the grassland. When the rainfall intensity reached the maximum at 13:50, the runoff occurrence rate of each plot also reached the maximum value. When the rainfall intensity gradually decreased to zero, the runoff ended. From the aspect of runoff rate, the order was grassland > apricot > corn > caragana. The grassland had a small area of grass cover, thus a small barrier to a runoff which subsequently resulted in a higher yield rate. The caragana and apricot fields had maximum vegetation coverage, which blocked the erosion due to rainfall, and lowered the runoff rate. Compared with the traditional farming method, the corn area makes better use of the land. In this rainfall, there is a gap between the plastic film mulching and the rainwater entering the corn, which increases the irrigation of rainwater to the plants in the shed and makes the yield flow rate lower (Figure 5a).

It can be seen from Figure 5b that the variation law of sediment yield and runoff yield in each plot tends to be consistent on the whole. In the first stage of rainfall, because of the small rainfall intensity, the only grassland started runoff and produced sediment, and the runoff and sediment yield rates were relatively low. In the second stage of rainfall, with the increase of rainfall intensity, the splash effect of raindrops on the surface was enhanced. When the soil water content reached saturation, the runoff rate increased rapidly, and the sediment carrying increased gradually, leading to increased sediment yield rate. The sediment yield rate also reached the maximum at 13:50 when the rainfall intensity reached the maximum, and then appeared a small fluctuation. The changing trend between the runoff rate and sediment yield was the same. According to the size of sediment yield rate, the order was grassland > corn > apricot > caragana. The sediment yield of the caragana field was the

lowest, which could be mainly due to the high coverage of caragana, which can better play the role of soil and water conservation and reduce the soil surface erosion caused by raindrops splashing. The sand yield rate of corn is lower than that of grassland but higher than apricot and caragana plots. As the corn plot is close to the greenhouse, the greenhouse makes the rainwater gather, and the splash ability of raindrops is greater than that of rainwater without accumulation, which makes the soil erosion degree relatively large around the greenhouse surface. Overall results showed that the caragana-field had the best effect on water and soil conservation, followed by the apricot tree field and corn plot.

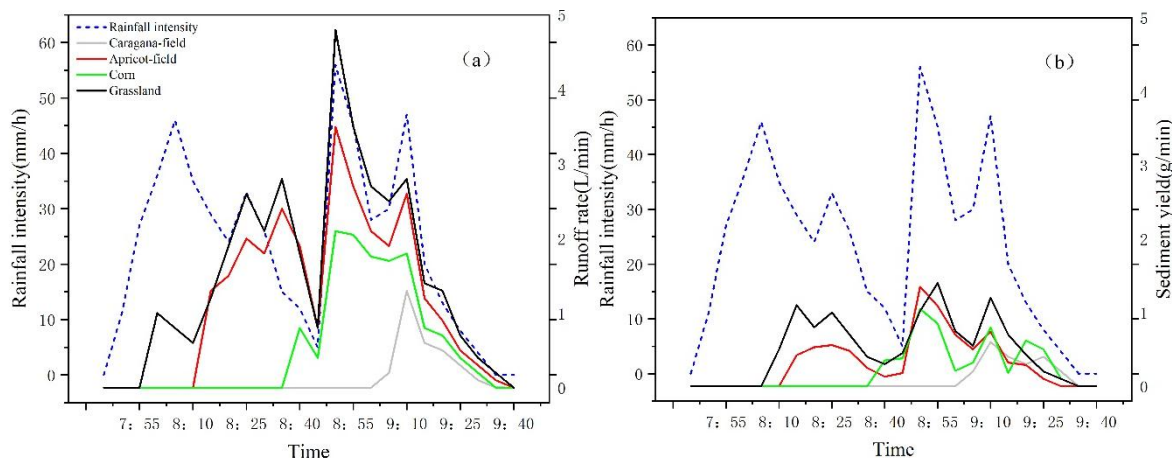


**Figure 5.** Characteristics of runoff (a) and sediment yield (b) under moderate rain conditions.

### 3.5. Analysis of runoff and sediment yield in different runoff plots

The runoff duration and the sediment production time of each field were basically consistent with those under heavy rain conditions (Table 5). Regarding total runoff and sediment yield, the order of runoff and sediment yield rate was grassland > corn > apricot > caragana. It was 3.9 times of the runoff and 2.8 times of the sediment yield of the caragana-field, 1.4 times and 1.5 times of the corn, 2.0 times and 1.8 times of the apricot-field. Under the condition of moderate rain, the soil and water conservation effect of caragana was still the best, followed by the apricot-field. Because of its low coverage rate and shallow root system, the ability of soil and water conservation was the weakest.

**Table 5.** Runoff and sediment yield characteristics of runoff plots under moderate rain.

Land-use	Duration of runoff generation (minutes)	Calendar time of sand production (minutes)	Production flow (L)	Sediment yield (g)
Caragana-field	160	145	8.72	3.30
Corn	210	195	23.8	6.00
Apricot-field	180	160	16.80	4.90
Grassland	240	224	34.00	9.20

#### 4. Discussion

There are many uncontrollable factors of natural rainfall, and the spatial and temporal distribution is uneven. This study adopted the method of natural rainfall, which is different from most artificial rainfall, and its practical significance is strengthened [27]. Under the condition of a rainstorm, the variation trend of runoff rate in different land-use systems was highly correlated with the changing trend of rainfall intensity, which is consistent with the previous research findings [28–32]. The occurrence time of the maximum values of runoff rate and sediment yield rates were basically the same as that of the maximum value of rainfall intensity. The greater the rainfall intensity, the earlier the maximum rates of runoff and sediments, which agrees with the findings of Mohamadi and Kavian [6] and Almeida et al. [33]. The caragana had the best effect on soil erosion control among the four different ecosystems because of its higher canopy interception [17,34]. Yue et al. [35] monitored the long-term impact of erosive rainstorm events on bare and vegetative lands and found that the vegetation restoration could reduce runoff by 68.0% to 97.4% and soil erosion by 98.0% to 99.9% compared to the bare lands. The results showed that the correlation between sediment yield and runoff rate was poor in the corn plot compared to the caragana, apricot, and grassland systems. While, compared with grassland, the runoff and sediment yield of corn were reduced by 30%–67% and 35%–47%, respectively. In general, the amount, intensity, and duration of rainfall all influence runoff and soil erosion. The surface runoff and soil erosion increased in different land-use types when rainfall levels exceeded soil infiltration rates [16]. Therefore, more intense rainfall and runoff events during the rainy season could result in increased soil and water erosion.

In the past, the government initiated a program named "Grain for Green" to address the environmental problems with economic sustainability [36]. Degraded lands were converted into forestation, shrubs, and grasslands [37–39]. Thus, the Yunwu Mountain has been protected [40]. Similarly, timely measures should be taken to conserve soil and water resources in the Qingshuihe watershed of the Changi district of the Zhangjiakou area [41,42].

#### 5. Conclusion

The findings of this study revealed that runoff and soil erosion rates were closely related to rainfall intensity and its erosivity. Comparing different land-use types, the caragana plantation or developing the corn industry would be conducive to conserving soil and water resources in the mountainous areas.

(1) The monthly rainfall of slope runoff plot in the Chongli mountain area presented the trend of concentrated rainfall in summer, mainly in June, July, August, and September, accounting for 83.47% of the total rainfall in 2014–2016, which was far higher than other months. From April to May every year, the rainfall increased with time, and the peak value of rainfall reached 160mm; from July to September, the rainfall gradually decreased, but it was still at a high level for the whole year.

(2) Caragana field can effectively reduce the kinetic energy of rainfall and runoff and reduce the runoff and sediment yield of slope compared to corn, apricot, and grassland systems. While greenhouse can make better use of rainfall for irrigation, reduce the erosion of bare farmland, and reduce the loss of farmland soil nutrients in the mountainous areas.

## Acknowledgments

This work was supported by the project “Mechanism of nitrogen migration in surface runoff and soil flow of sloping farmland in Miyun Reservoir” (QNJJ202214), “optimization and application of ecological prevention and control mode of non-point source pollution in Miyun reservoir water source protection area” (YZS201910) and Beijing Rural Revitalization science and technology project “Experimental demonstration of key techniques for planting forest medicine for soil fixation and water conservation in Yuanshan area”.

## Conflict of interest

The authors declare no conflict of interest.

## References

1. Bouguerra S, Jebari S, Tarhouni J (2020) Spatiotemporal analysis of landscape patterns and its effect on soil loss in the Rmel river basin, Tunisia. *Soil and Water Research* 16: 39–49. <http://doi.org/10.17221/84/2019-SWR>
2. Flores BM, Staal A, Jakovac CC, et al. (2020) Correction to: Soil erosion as a resilience drain in disturbed tropical forests. *Plant and Soil* 450: 27–28. <http://doi.org/10.1007/s11104-019-04286-5>
3. Thapa P (2020) Spatial estimation of soil erosion using RUSLE modeling: a case study of Dolakha district, Nepal. *Environmental Systems Research* 9: 1–10. <http://doi.org/10.1186/s40068-020-00177-2>
4. Keesstra S, Mol G, De Leeuw J, et al. (2018) Soil-related sustainable development goals: Four concepts to make land degradation neutrality and restoration work. *Land* 7: 133. <http://doi.org/10.3390/land7040133>
5. Keesstra S, Sannigrahi S, López-Vicente M, et al. (2021) The role of soils in regulation and provision of blue and green water. *Philosophical Transactions of the Royal Society B* 376: 20200175. <http://doi.org/10.1098/RSTB.2020.0175>
6. Mohamadi MA, Kavian A (2015) Effects of rainfall patterns on runoff and soil erosion in field plots. *International soil and water conservation research* 3 : 273–281. <http://doi.org/10.1016/j.iswcr.2015.10.001>
7. Zhao B, Zhang L, Xia Z, et al. (2019) Effects of rainfall intensity and vegetation cover on erosion characteristics of a soil containing rock fragments slope. *Advances in civil engineering* 2019. <https://doi.org/10.1155/2019/7043428>
8. Sartori M, Philippidis G, Ferrari E, et al. (2019) A linkage between the biophysical and the economic: Assessing the global market impacts of soil erosion. *Land use policy* 86: 299–312. <https://doi.org/10.1016/j.landusepol.2019.05.014>
9. Montanarella L, Badraoui M, Chude V, et al. (2015) Status of the world's soil resources: main report. *Embrapa Solos-Livro científico (ALICE)*.
10. Cai M, An C, Guy C, et al. (2020) Assessment of soil and water conservation practices in the loess hilly region using a coupled rainfall-runoff-erosion model. *Sustainability* 12: 934. <https://doi.org/10.3390/su12030934>

11. Visconti D, Fiorentino N, Cozzolino E, et al. (2020) Use of giant reed (*Arundo donax* L.) to control soil erosion and improve soil quality in a marginal degraded area. *Italian Journal of Agronomy* 15: 332–338. <https://doi.org/10.4081/ija.2020.1764>
12. Shi P, Schulin R (2018) Erosion-induced losses of carbon, nitrogen, phosphorus and heavy metals from agricultural soils of contrasting organic matter management. *Science of the Total Environment* 618: 210–218. <https://doi.org/10.1016/j.scitotenv.2017.11.060>
13. Fiener P, Auerswald K, Van Oost K (2011) Spatio-temporal patterns in land use and management affecting surface runoff response of agricultural catchments—A review. *Earth-Science Reviews* 106: 92–104. <https://doi.org/10.1016/j.earscirev.2011.01.004>
14. Worrall F, Burt TP, Howden N J (2016) The fluvial flux of particulate organic matter from the UK: the emission factor of soil erosion. *Earth Surface Processes and Landforms* 41: 61–71. <https://doi.org/10.1002/esp.3795>
15. Berhe AA, Harden JW, Torn MS, et al. (2008) Linking soil organic matter dynamics and erosion - induced terrestrial carbon sequestration at different landform positions. *Journal of Geophysical Research: Biogeosciences* 113. <https://doi.org/10.1029/2008JG000751>
16. She D, Liu Y, Shao MA, et al. (2012) Simulated effects and adaptive evaluation of different canopies rainfall interception models in Loess Plateau. *Transactions of the Chinese Society of Agricultural Engineering* 28: 115–120.
17. Guo Z, Shao M (2013) Impact of afforestation density on soil and water conservation of the semiarid Loess Plateau, China. *Journal of Soil and water conservation* 68: 401–410. <https://doi.org/10.2489/jswc.68.5.401>
18. Wang L, Xie J, Luo Z, et al. (2021). Forage yield, water use efficiency, and soil fertility response to alfalfa growing age in the semiarid Loess Plateau of China. *Agricultural Water Management* 243: 106415. <https://doi.org/10.1016/j.agwat.2020.106415>
19. Zhao H, He H, Wang J, et al. (2018) Vegetation restoration and its environmental effects on the Loess Plateau. *Sustainability* 10: 4676. <https://doi.org/10.3390/su10124676>
20. Pan T, Zuo L, Zhang Z, et al. (2020) Impact of land use change on water conservation: a case study of Zhangjiakou in Yongding River. *Sustainability* 13: 22. <https://doi.org/10.3390/SU13010022>
21. Chu X, Deng X, Jin G, et al. (2017) Ecological security assessment based on ecological footprint approach in Beijing-Tianjin-Hebei region, China. *Physics and Chemistry of the Earth* 101: 43–51. <https://doi.org/10.1016/j.pce.2017.05.001>
22. Li M, Yao W, Shen Z, et al. (2016) Erosion rates of different land uses and sediment sources in a watershed using the<sup>137</sup>Cs tracing method: Field studies in the Loess Plateau of China. *Environmental Earth Sciences* 75: 1–10. <https://doi.org/10.1007/s12665-015-5225-6>
23. Cerdà A, Novara A, Moradi E. (2021) Long-term non-sustainable soil erosion rates and soil compaction in drip-irrigated citrus plantation in Eastern Iberian Peninsula. *Science of the Total Environment* 787: 147549. <https://doi.org/10.1016/J.SCITOTENV.2021.147549>.
24. Rodrigo Comino J, Keesstra SD, Cerdà A (2018) Connectivity assessment in Mediterranean vineyards using improved stock unearthing method, LiDAR and soil erosion field surveys. *Earth Surface Processes and Landforms* 43: 2193–2206. <https://doi.org/10.1002/esp.4385>
25. Keesstra SD, Davis J, Masselink RH, et al. (2019) Coupling hysteresis analysis with sediment and hydrological connectivity in three agricultural catchments in Navarre, Spain. *Journal of Soils and Sediments* 19: 1598–1612. <https://doi.org/10.1007/s11368-018-02223-0>

26. Cerdà Artemi TE, Daliakopoulos IN (2021) Weed cover controls soil and water losses in rainfed olive groves in Sierra de Enguera, eastern Iberian Peninsula. *Journal of Environmental Management* 290: 112516. <https://doi.org/10.1016/J.JENVMAN.2021.112516>.
27. Wang X, He K, Dong Z (2019) Effects of climate change and human activities on runoff in the Beichuan River Basin in the northeastern Tibetan Plateau, China. *Catena* 176: 81–93. <https://doi.org/10.1016/j.catena.2019.01.001>
28. Fang NF, Wang L, Shi ZH (2017) Runoff and soil erosion of field plots in a subtropical mountainous region of China. *Journal of Hydrology* 552: 387–395. <https://doi.org/10.1016/j.jhydrol.2017.06.048>
29. Chen H, Zhang X, Abla M, et al. (2018) Effects of vegetation and rainfall types on surface runoff and soil erosion on steep slopes on the Loess Plateau, China. *Catena* 170: 141–149. <https://doi.org/10.1016/j.catena.2018.06.006>
30. Deng L, Kim DG, Li M, et al. (2019) Land-use changes driven by 'Grain for Green' program reduced carbon loss induced by soil erosion on the Loess Plateau of China. *Global and planetary change* 177: 101–115. <https://doi.org/10.1016/j.gloplacha.2019.03.017>
31. Bogale A, Aynalem D, Adem A, et al. (2020) Spatial and temporal variability of soil loss in gully erosion in upper Blue Nile basin, Ethiopia. *Applied Water Science* 10: 1–8. <https://doi.org/10.1007/s13201-020-01193-4>.
32. Sun C, Hou H, Chen W (2021) Effects of vegetation cover and slope on soil erosion in the Eastern Chinese Loess Plateau under different rainfall regimes. *PeerJ* 9: e11226. <https://doi.org/10.7717/PEERJ.11226>.
33. de Almeida WS, Seitz S, de Oliveira LFC, et al. (2021). Duration and intensity of rainfall events with the same erosivity change sediment yield and runoff rates. *International Soil and Water Conservation Research* 9: 69–75. <https://doi.org/10.1016/j.iswcr.2020.10.004>.
34. Zeng Q, Lal R, Chen Y, et al. (2017) Soil, leaf and root ecological stoichiometry of *Caragana korshinskii* on the Loess Plateau of China in relation to plantation age. *PLoS One* 12: e0168890. <https://doi.org/10.1371/journal.pone.0168890>.
35. Liang Y, Jiao JY, Tang BZ, et al. (2020) Response of runoff and soil erosion to erosive rainstorm events and vegetation restoration on abandoned slope farmland in the Loess Plateau region, China. *Journal of Hydrology* 584: 124694. <https://doi.org/10.1016/j.jhydrol.2020.124694>.
36. Chen X, Zhang X, Zhang Y, et al. (2009) Carbon sequestration potential of the stands under the Grain for Green Program in Yunnan Province, China. *Forest Ecology and Management* 258: 199–206. <https://doi.org/10.1016/j.foreco.2008.07.010>
37. Wolf B, Kiese R, Chen W, et al. (2012) Modeling N2O emissions from steppe in Inner Mongolia, China, with consideration of spring thaw and grazing intensity. *Plant and soil* 350: 297–310. <https://doi.org/10.1007/s11104-011-0908-6>
38. Deng L, Liu GB, Shangguan ZP (2014) Land - use conversion and changing soil carbon stocks in China's 'Grain - for - Green'Program: a synthesis. *Global Change Biology* 20: 3544–3556. <https://doi.org/10.1111/gcb.12508>
39. Wang D, Liu Y, Shang ZH, et al. (2015). Effects of grassland conversion from cropland on soil respiration on the semi - arid loess plateau, China. *CLEAN–Soil, Air, Water* 43: 1052–1057. <https://doi.org/10.1002/clen.201300971>

40. Cheng J, Cheng J, Hu T, et al. (2012) Dynamic changes of *Stipa bungeana* steppe species diversity as better indicators for soil quality and sustainable utilization mode in Yunwu Mountain Nature Reserve, Ningxia, China. *CLEAN–Soil, Air, Water* 40: 127–133. <https://doi.org/10.1002/clen.201000438>
41. Tang L, Zhang Z, Wang X, et al. (2010) Effects of precipitation and land use/cover variability on erosion and sediment yield in Qingshuihe Watershed on the Loess Plateau. China. *J Nat Resour* 8.
42. Zhu KB, Li ZH, Yang SP (2014) Features and Assessment of Ecological Restoration Models of Qingshuihe Watershed in Rainstorm Center Area. *Bulletin of Soil & Water Conservation* 4: 193–197.



AIMS Press

© 2022 the Author(s), licensee AIMS Press. This is an open access article distributed under the terms of the Creative Commons Attribution License (<http://creativecommons.org/licenses/by/4.0>)